Progress In Electromagnetics Research M, Vol. 13, 217–227, 2010

ANALYSIS OF CHARACTERISTICS OF TWO-DIMENSIONAL RUNGE-KUTTA MULTIRESOLUTION TIME-DOMAIN SCHEME

X. Chen and Q. Cao

College of Information Science & Technology
Nanjing University of Aeronautics and Astronautics
Nanjing 210016, China

Abstract—In this paper, the stability condition of the Runge-Kutta m-order multiresolution time-domain (RKm-MRTD) scheme has been studied. By analyzing the amplification factors, we derive the numerical dispersion relation of the RK-MRTD scheme. The numerical dispersive and dissipative errors are investigated. Finally, the theoretical predictions of the numerical errors are calculated through the numerical simulations.

1. INTRODUCTION

The multiresolution time-domain (MRTD) method for the numerical simulation of solutions to Maxwell's electromagnetic equations was initially introduced in 1996 [1], which had selected the popular and classical finite difference time-domain (FDTD) approach as alternative. It has been shown obviously that the MRTD scheme has advantages in memory and CPU time compared with the FDTD method and has been used to solve many electromagnetic problems [2–4]. The typical MRTD scheme has been proven to have the potential of the high order convergence in space. However, in these typical implementations, the realization of this potential is hindered by a low-order (leap-frog) time-stepping procedure. Using the SSP-RK method, which was first introduced in [5] and extended in [6] and which achieves full high-order convergence in time and space while keeping the time-step proportional to the spatial mesh-size. Normally, the basis functions used in the RK-MRTD method are the compactly supported N-order wavelets (e.g., the Daubechies DN functions) and m chosen the same as N.

Corresponding author: Q. Cao (qunsheng@nuaa.edu.cn).

Theoretically, the RK-MRTD method has the high order convergence in both space and time [7].

In this paper, we dedicate to analyze the stability condition, numerical dispersive and dissipative errors of the RK-MRTD method in two-dimensional case.

The remainder of the paper is organized as follows. First, in Section 2, we review the basic equations and concepts related to the RK-MRTD scheme. Second, in Section 3, the numerical properties of the method are represented including the stability condition, numerical dispersive and dissipative errors characteristics. And then, in Section 4, we provide the example and results of the numerical simulations. Finally, the conclusions are summarized in Section 5.

2. RK-MRTD SCHEME

For the RKm-MRTD method, namely, the m-order RK-MRTD method, completing the spatial discretization and using the Daubechies function as the scaling function DN ($N = m$), the resulting semidiscrete form of Maxwell's equation can be symbolically written [7] as

$$\frac{\partial \mathbf{F}}{\partial t} = \mathbf{L}\mathbf{F} + S(t), \tag{1}$$

where $\mathbf{F} = \begin{Bmatrix} \mathbf{E} \\ \mathbf{H} \end{Bmatrix}$, the components $\mathbf{E}$ and $\mathbf{H}$ are expressed as $\mathbf{E} = \begin{Bmatrix} E_x \\ E_y \\ E_z \end{Bmatrix}$, $\mathbf{H} = \begin{Bmatrix} H_x \\ H_y \\ H_z \end{Bmatrix}$, respectively, and the operator $\mathbf{L}$ is defined as $\mathbf{L} = \begin{bmatrix} 0 & L_H \\ L_E & 0 \end{bmatrix}$ and $S(t)$ is a source connected with time variable. Eq. (1) is discretized with an mth-order m stage strong stability preserving Runge-Kutta (SSP-RK) method with low storage requirements [5–7], and

$$\begin{aligned} &F^{(0)} = F(t_n) \\ &F^{(i)} = F^{(i-1)} + \Delta t L \cdot F^{(i-1)} + \Delta t S^i, \quad i = 1, 2, \ldots, m \\ &F(t_{n+1}) = \sum_{l=0}^{m} \alpha_{m,l} F^{(l)} \end{aligned}, \tag{2}$$

where $S^{(i)} = (I + \Delta t\frac{\partial}{\partial t})^{\mathrm{i}-1} S(t_n)$, $i = 1, \ldots, m$, and the coefficients $\alpha_{i,j}$ [5–7] are

$$\begin{aligned} \alpha_{m,m} &= \frac{1}{m!}, \quad l = m \\ \alpha_{m,l} &= \frac{1}{l}\alpha_{m-1,l-1}, \quad l = 1, 2, \ldots, m-1,\ m \geq 2 \\ \alpha_{m,0} &= 1 - \sum_{l=1}^{m} \alpha_{m,l}, \quad l = 0 \end{aligned} \tag{3}$$

3. NUMERICAL PROPERTIES FOR RK-MRTD SCHEME

Now, we use the Fourier method [8] to analyze the stability, dispersive and dissipative characteristics of the RK-MRTD method. As an example, we consider a two-dimensional TMz wave in an isotropic loss-free medium. The update equations for the TMz wave in the RK-MRTD scheme is,

$$\begin{aligned} \frac{\partial_z E_{I,J}(t)}{\partial t} &= +\frac{1}{\varepsilon}\sum_{\upsilon} a(\upsilon)\left[{}_yH_{I+\frac{1}{2}+\upsilon,J}(t)\frac{1}{\Delta x} - {}_xH_{I,J+\frac{1}{2}+\upsilon}(t)\frac{1}{\Delta y}\right] \\ \frac{\partial_x H_{I,J+\frac{1}{2}}(t)}{\partial t} &= -\frac{1}{\mu\Delta y}\sum_{\upsilon} a(\upsilon)\,{}_zE_{I,J+1+\upsilon}(t) \\ \frac{\partial_y H_{I+\frac{1}{2},J}(t)}{\partial t} &= +\frac{1}{\mu\Delta x}\sum_{\upsilon} a(\upsilon)\,{}_zE_{I+1+\upsilon,J}(t) \end{aligned} \tag{4}$$

where I and J are the spatial indexes. Δx and Δy are the spatial increments along the x- and y-directions, respectively. The $\alpha(\upsilon)$ are the expansion coefficients for the Daubechies scaling functions, and the coefficient satisfies the symmetry condition $\alpha(\upsilon) = -\alpha(-\upsilon - 1)$. The values of $\alpha(\upsilon)$ can be found in [7].

The trial solutions of the fields for the TMz wave are,

$$\begin{aligned} {}_zE_{I,J}(t) &= E_z(t)e^{j(k_xI\Delta x + k_yJ\Delta y)} \\ {}_xH_{I,J+1/2}(t) &= H_x(t)e^{j\left[k_xI\Delta x + k_y(J+\frac{1}{2})\Delta y\right]}, \\ {}_yH_{I+1/2,J}(t) &= H_y(t)e^{j\left[k_x(I+\frac{1}{2})\Delta x + k_yJ\Delta y\right]} \end{aligned} \tag{5}$$

where k_x and k_y are, respectively, the computed numerical wavenumbers in the x- and y-directions. The Fourier analysis can be performed by substituting Eq. (5) into Eq. (4). We have obtained

the following equation,

$$\frac{\partial}{\partial t}\begin{bmatrix} E_z(t) \\ H_x(t) \\ H_y(t) \end{bmatrix} = \mathbf{L}\begin{bmatrix} E_z(t) \\ H_x(t) \\ H_y(t) \end{bmatrix}, \tag{6}$$

where the term $\mathbf{L}$, called the spatial amplification matrix, is defined as

$$\mathbf{L} = \begin{bmatrix} 0 & L_1 & L_2 \\ L_3 & 0 & 0 \\ L_4 & 0 & 0 \end{bmatrix}, \tag{7}$$

and

$$L_1 = -\frac{2j\sum_{v=0}^{N} a(v)\sin\left(k_y\left(\frac{1}{2}+v\right)\Delta y\right)}{\varepsilon\Delta y}, \tag{8a}$$

$$L_2 = \frac{2j\sum_{v=0}^{N} a(v)\sin\left(k_x\left(\frac{1}{2}+v\right)\Delta x\right)}{\varepsilon\Delta x}, \tag{8b}$$

$$L_3 = -\frac{2j\sum_{v=0}^{N} a(v)\sin\left(k_y\left(\frac{1}{2}+v\right)\Delta y\right)}{\mu\Delta y}, \tag{8c}$$

$$L_4 = \frac{2j\sum_{v=0}^{N} a(v)\sin\left(k_x\left(\frac{1}{2}+v\right)\Delta x\right)}{\mu\Delta x}. \tag{8d}$$

In order to obtain the solution of the matrix $\mathbf{L}$, we use the following eigen equation to find the eigen-values of $\mathbf{L}$.

$$|\lambda I - \mathbf{L}| = \lambda^3 - \lambda\left(\left(\frac{2jc\sum_{v=0}^{N} a(v)\sin\left(k_x\left(\frac{1}{2}+v\right)\Delta x\right)}{\Delta x}\right)^2 + \left(\frac{2jc\sum_{v=0}^{N} a(v)\sin\left(k_y\left(\frac{1}{2}+v\right)\Delta y\right)}{\Delta y}\right)^2\right) = 0 \tag{9}$$

For the MRTD scheme (including the FDTD method), the eigen-values

λ are pure imaginary or zero. The positive ones are

$$\lambda = j2c\sqrt{\left(\frac{\sum_{v=0}^{N} a(v)\sin\left[k_x\left(\frac{1}{2}+v\right)\Delta x\right]}{\Delta x}\right)^2+\left(\frac{\sum_{v=0}^{N} a(v)\sin\left[k_y\left(\frac{1}{2}+v\right)\Delta y\right]}{\Delta y}\right)^2} = j\lambda_i \tag{10}$$

where c is the physical velocity, and λ_i is the imaginary part of λ.

Further, Eq. (2) can be rewritten as the following [5],

$$F(t_{n+1}) = \sum_{l=0}^{m} \frac{1}{l!}(\Delta t\mathbf{L})^l F(t_n) = \mathbf{G}F(t_n), \tag{11}$$

where $\mathbf{G}$ is the total amplification matrix including the influence of the time discretization. The eigen-values of $\mathbf{G}$ are the amplification factor $\boldsymbol{\sigma}$.

For the RKm time integrations, the factor σ is obtained

$$\sigma_{\mathrm{RKm}} = \sum_{l=0}^{m} \frac{1}{l!}(\lambda\Delta t)^l. \tag{12}$$

For leapfrog time integration [9], the factor σ is

$$\sigma_{\mathrm{leapforg}} = 1 + \frac{1}{2}(\lambda\Delta t)^2 \pm \sqrt{\left[1+\frac{1}{2}(\lambda\Delta t)^2\right]^2 - 1}. \tag{13}$$

Here, λ in Eqs. (12) and (13) are obtained by Eq. (7).

The modulus of σ determines the stability and dissipative error, and the argument determines the combined dispersive error caused by the spatial and time discretization [8].

3.1. Stability Condition of RK-MRTD

It is clear that if the numerical methods are stable, then it means $|\sigma| \leq 1$. It is easily shown that we can draw $\lambda_i\Delta t \leq C_t$, and the constant C_t is related to the time-stepping scheme. For example, if $m = 3$, we have $|\sigma| \leq 1$, then

$$\begin{aligned}\left|\sum_{l=0}^{3}\frac{1}{l!}(\lambda\Delta t)^l\right| &= \left|\sum_{l=0}^{3}\frac{1}{l!}(j\lambda_i\Delta t)^l\right| \\ &= \left|1+(j\lambda_i\Delta t)-\frac{1}{2}(\lambda_i\Delta t)^2+\frac{1}{6}(\lambda_i\Delta t)^3\right| \leq 1\end{aligned}$$

Table 1. Coefficient C_t for different time-stepping schemes.

	leapfrog	RK1	RK2	RK3	RK4
C_t	2	0	0	$\sqrt{3}$	$2\sqrt{2}$

Table 2. The CFL number α for different time-stepping schemes.

	FDTD	MRTD (D2)	RK3-MRTD	RK4-MRTD
α (2D)	0.7071	0.5303	0.4191	0.6585
α (3D)	0.5774	0.4330	0.3422	0.5377

Further, $\left|1 + (j\lambda_i\Delta t) - \frac{1}{2}(\lambda_i\Delta t)^2 + \frac{1}{6}(\lambda_i\Delta t)^3\right| \leq 1$. Finally, we have $(\lambda_i\Delta t) \leq \sqrt{3}$.

If one assumes a uniform grid spacing, $\Delta x = \Delta y = \Delta s$, then we can derive the stability condition the same as [10],

$$\Delta t \leq \frac{C_t}{\sqrt{d}\sum_{v=-N-1}^{N}|a(v)|}\frac{\Delta s}{c} = \alpha\frac{\Delta s}{c},$$

where α is the CFL number, and $d = 1, 2, 3$ is the dimensionality. Here d is 2.

According to Table 1, RK1-MRTD and RK2-MRTD are unconditionally unstable. However, if $m \geq 3$, it is possible for the RKm-MRTD schemes to be conditionally stable.

As can be seen from Table 2, the third-order RK-MRTD method requires a harsher stability condition and a smaller time step than the MRTD (D2) method, but the stability condition of the fourth-order RK-MRTD method is looser than MRTD (D2).

3.2. Dispersive Characteristic

According to [11], by substituting Eq. (7) into the following equation,

$$\omega t = Arg(\sigma), \tag{14}$$

we can obtain the numerical dispersion relation of the RKm-MRTD scheme, where ω is angular frequency.

Substitution of the following relations, $\omega = \frac{2\pi}{\lambda_c}c$, $k_x = k_p\cos(\theta) = \frac{2\pi}{\lambda_p}\cos(\theta)$, $k_y = k_p\sin(\theta) = \frac{2\pi}{\lambda_p}\sin(\theta)$, $N_c = \frac{\lambda_c}{\Delta s}$, $\Delta t = \alpha\Delta s/c$ into Eq. (13). Finally, we have obtained a function of variables N_c, λ_c/λ_p, θ and α, where N_c is the number of cells per wavelength; λ_c is the theoretical wavelength in the continuous medium; λ_p is the numeric

wavelength; and θ is the direction of wave propagation that is relative to the x-axis.

The RKm-MRTD scheme exhibits a more highly linear numerical dispersion performance than that of the standard MRTD method, shown in Figs. 1 and 2. And the higher order of the scheme is, the more highly linear numerical dispersion performance becomes. It is consistent with the error analysis for the order in [7]. The angle $\theta = \pi/2$ is the direction of the largest dispersive error, but the angle $\theta = \pi/4$ is for the least one.

3.3. Dissipative Characteristic

When the stability condition is satisfied for the RK3-MRTD and RK4-MRTD methods, $|\sigma|$ is not always equal to 1, so they exist dissipatively.

It is known that λ is pure imaginary, then the dissipative error of the high order method is caused by the time discretization. Because of the anisotropy of the spatial discretization error and the isotropy of the time discretization error, the overall dissipative error still has a slight anisotropic characteristic. From Figs. 3 and 4, it is found that the dissipative errors are very small and increase with the decrease of N_c. And the dissipative error of the RK4-MRTD scheme is much smaller than that of the one caused by the RK3-MRTD scheme.

4. NUMERICAL RESULTS

In order to compare with the results from the different order in the RK-MRTD method, we study a 2D parallel plate resonator with total size 1 m × 1 m and $\Delta x = \Delta y = \Delta s = 0.1$ m, and analyze the TMz

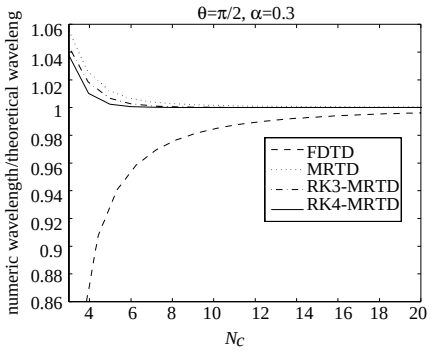

Figure 1. Dispersion performance for $\theta = \pi/2$.

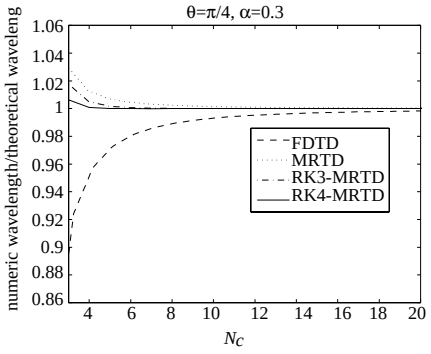

Figure 2. Dispersion performance for $\theta = \pi/4$.

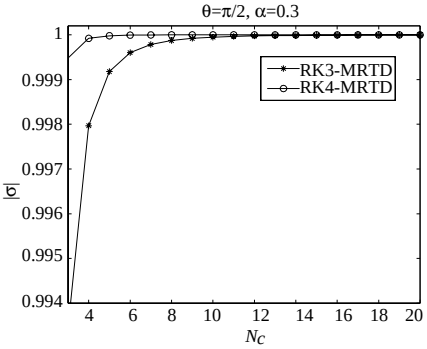

Figure 3. The dissipative errors for $\theta = \pi/2$.

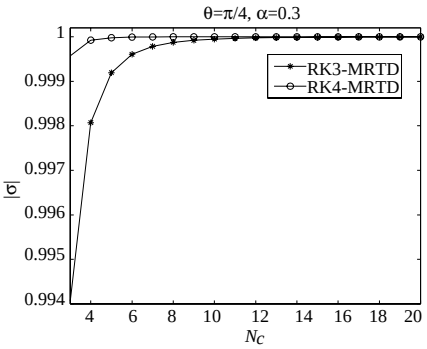

Figure 4. The dissipative errors for $\theta = \pi/4$.

Table 3. Resonant frequency in an empty cavity resolved by different modes (N_c = cells/modal wavelength).

Mode	Analytic (GHz)	FDTD		MRTD		RK3-MRTD		RK4-MRTD		N_c
		Values	Error	Values	Error	Values	Error	Values	Error	
(1,1)	0.2121	0.2116	–0.23%	0.2124	0.13%	0.2122	0.06%	0.2122	0.06%	14.1421
(1,3)	0.4743	0.4604	–2.95%	0.4778	0.72%	0.4752	0.17%	0.4745	0.04%	6.2346
(3,3)	0.6364	0.6171	–3.04%	0.6430	1.04%	0.6380	0.25%	0.6366	0.03%	4.7140
(3,5)	0.8746	0.8113	–7.24%	0.8955	2.39%	0.8887	1.60%	0.8810	0.73%	3.4300

polarization model. The CFL number α is chosen as 0.3, which means the time increment $\Delta t = 1.0 \times 10^{-10}$ s. Assume $\varepsilon = \varepsilon_0$, $\mu = \mu_0$, and the unit impulse is excited at the grid point (5, 5). The total simulation time is $2^{15}\Delta t$, and the values of the electric field E have been recorded as time series. The resonant frequencies have been shown in Fig. 5 for the different modes. Fig. 6 shows the convergence of the 2D rectangular cavity, and we test the frequency error in mode (1, 1).

From Table 3, it is found that the errors are increased with increasing frequency and also rapidly decreased with the increments of the order of the method we used. When N_c is changed from 4 to 3, the errors of the higher-order methods have a rapid change. And all of these characteristics coincide with the dispersion curve. If the error requirement is chosen 0.72%, then the RK4-MRTD mode takes about 3 grids per wavelength, and the normal MRTD scheme needs six grids, but the FDTD method requires about 10 grids. If the error requirement is 0.03%, then the advantages of the higher-order methods are more obvious in reducing memory requirement and computational cost. As a dissipative result of the higher-order methods, it is found

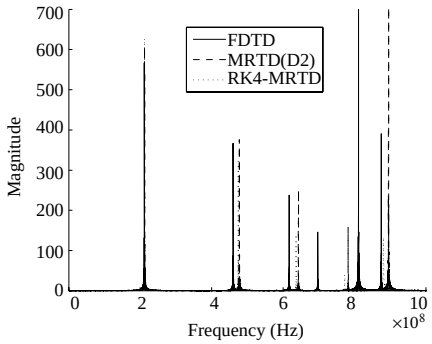

Figure 5. The Resonant frequencies for different modes.

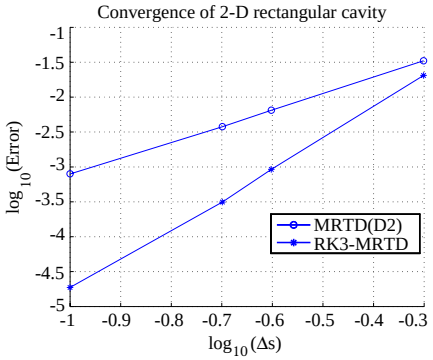

Figure 6. Convergence of the MRTD (D2) and the RK-MRTD (D3, $m = 3$) schemes for a 2D rectangular waveguide case.

that the magnitude of the RK4-MRTD spectrum gradually decreases with the increment of frequency shown in Fig. 5, which coincides with the results shown in Figs. 3 and 4.

Now, we analyze memory requirement and computational cost. For a certain problem with the same mesh, for the 2D case, the memory requirements of the RKm-MRTD are 7/3 times of the requirements of the MRTD/FDTD method, because the storage needed for E is different from H. But for the 1D and 3D problems, the multiplier is 2.5. However, for a given accuracy, the RKm-MRTD will cost less memory than the conventional MRTD. Furthermore, because we have given the stability conditions of the RK-MRTD method, the estimated time consumption reported [7] requires a slight amendment. And Eq. (7) in [7] needs to be amended as follows:

$$(n_2)^{1-\frac{2}{N}} > (Q_{d,N})^{\frac{2}{N}} \sqrt[d+1]{\frac{\alpha_2}{\alpha_m} \cdot \frac{N}{\gamma} \cdot \frac{4N-1}{4N-2}}, \tag{15}$$

where $n_2 = 1/\Delta x_2, N$ is the order of the RK-MRTD method that we use. The dimensionality constant $d = 1; 2; 3$ for 1D, 2D and 3D, respectively, and γ is a given constant. The significance of the symbolic in Eq. (15) is the same as in [7]. And $Q_{d,N}$ can be calculated [7] by the following Equation (16):

$$Q_{d,N} = \frac{\Delta x_2}{(\Delta x_N)^{N/2}}, \tag{16}$$

where Δx_N is the grid spacing of the order N in the method, and Δx_2 denotes the grid spacing of the conventional MRTD method.

According to Eq. (15), for a given CFL number α_2, α_m and γ, when n_2 is more than a certain numerical value, the computational time of the RK-MRTD method will just be γ times of the MRTD method. The constants $Q_{d,N}$ in (15) can be estimated by Eq. (16), and for the above numerical simulation example we use the results described in Fig. 6 to get the value $Q_{2,3} = 0.9642$.

5. CONCLUSION

In this paper, we have analyzed some numerical characteristics of the 2D RK-MRTD scheme, which includes the stability property, numerical dispersive and dissipative errors using the Fourier analysis method. We have verified by the simulations and presented an estimation method for the computational time and memory. It is found that the RKm-MRTD modes have better dispersion characteristics, in particular, and the RK4-MRTD mode has looser conditions of the stability than those of the normal MRTD method. The RKm-MRTD modes are dissipative, but also consume 2.5 times of the memory, and more than m times of the computational time for the same grid. It is obvious that when high precision is required, the RK-MRTD methods' advantages can be clearly demonstrated. But in the application of the RK-MRTD scheme, the theoretical model should be in high-precision too. Therefore, the expansion in the scope of its application is still facing many challenges.

ACKNOWLEDGMENT

The work was supported by the National Natural Science Foundation of China under Contract 60771018.

REFERENCES

1. Krumpholz, M. and L. P. B. Katehi, "MRTD: New time-domain schemes based on multiresolution analysis," *IEEE Trans. Microw. Theory Tech.*, Vol. 44, No. 4, 555–571, Apr. 1996.
2. Cao, Q., Y. Chen, and R. Mittra, "Multiple image technique (MIT) and anisotropic perfectly matched layer (APML) in implementation of MRTD scheme for boundary truncations of microwave structures," *IEEE Trans. Microw. Theory Tech.*, Vol. 50, No. 6, 1578–1589, Jun. 2002.
3. Zhu, X., T. Dogaru, and L. Carin, "Analysis of the CDF biorthogonal MRTD method with application to PEC targets,"

IEEE Trans. Microw. Theory Tech., Vol. 51, No. 9, 2015–2022, Sep. 2003.

4. Alighanbari, A. and C. D. Sarris, "Dispersion properties and applications of the Coifman scaling function based S-MRTD," *IEEE Trans. Antennas and Propagation*, Vol. 54, No. 8, 2316–2325, Aug. 2006.
5. Gottlieb, S., C.-W. Shu, and E. Tadmor, "Strong stability-preserving high-order time discretization methods," *SIAM Rev.*, Vol. 43, No. 1, 89–112, 2001.
6. Chen, M.-H., B. Cockburn, and F. Reitich, "High-order RKDG methods for computational electromagnetics," *J. Sci. Comput.*, Vol. 22/23, No. 1–3, 205–226, Jun. 2005.
7. Cao, Q., R. Kanapady, and F. Reitich, "High-order Runge-Kutta multiresolution time-domain methods for computational electromagnetics," *IEEE Trans. Microw. Theory Tech.*, Vol. 54, No. 8, 3316–3326, Aug. 2006.
8. Liu, Y., "Fourier analysis of numerical algorithms for the Maxwell's equations," *J. Comput. Phys.*, Vol. 124, 396–416, 1996.
9. Yefet, A. and P. G. Petropoulos, "A non-dissipative staggered fourth-order accurate explicit finite difference scheme for the time-domain Maxwell's equations," *Sci. Eng., Tech. Rep.*, Inst. Comput. Applicat, NASA/CR-1999\-209\514, 1999.
10. Shan, Z. and G. W. Wei, "High-order FDTD methods via derivative matching for Maxwell's equations with material interface," *J. Comput. Phys.*, Vol. 200, No. 1, 60–103, Oct. 2004.
11. Sun, G. and C. W. Trueman, "Analysis and numerical experiments on the numerical dispersion of two-dimensional ADI-FDTD," *IEEE Antenna and Wireless Propagation Lett.*, Vol. 2, No. 7, 78–81, 2003.